RSC Advances



This is an *Accepted Manuscript*, which has been through the Royal Society of Chemistry peer review process and has been accepted for publication.

Accepted Manuscripts are published online shortly after acceptance, before technical editing, formatting and proof reading. Using this free service, authors can make their results available to the community, in citable form, before we publish the edited article. This Accepted Manuscript will be replaced by the edited, formatted and paginated article as soon as this is available.

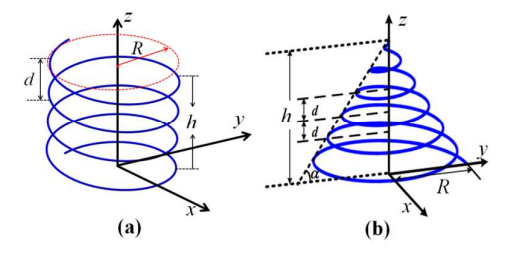
You can find more information about *Accepted Manuscripts* in the **Information for Authors**.

Please note that technical editing may introduce minor changes to the text and/or graphics, which may alter content. The journal's standard <u>Terms & Conditions</u> and the <u>Ethical guidelines</u> still apply. In no event shall the Royal Society of Chemistry be held responsible for any errors or omissions in this *Accepted Manuscript* or any consequences arising from the use of any information it contains.



Table of Contents entry

A geometric model for describing the kinetic growth of helical structures is derived and the correlation between helix length with parameters including height, pitch and radius is evaluated.



Length evolution of helical micro/nano-scale structures

Yuanqiang Song^{1†}, Xian Jian^{1†}, Pan Yu^{1†}, Bo Wang², Weirong Huo¹, Aifang Liu¹, Weiqiang Lv¹ & Weidong He^{1,3,4*}

Abstract

Helical structures frequently exist in nature, and two commonly-seen examples are the curly hair of humans and the helical fujiko of luffa. Helical micro/nanoscale crystals have evolved to be an increasingly-intriguing form of crystals since its first—cited observation more than half a century ago. In addition to carbon, a number of other materials have also been found to form helical structure spontaneously or in the presence of metallic catalysts. In the special shape with extensive lattice strain, typically triggering a variety of unusual properties, makes such crystals of particular interest to the materials field. Up to this point, the growth kinetics of such helical nanocrystals still remains elusive. To resolve the growth kinetics, one must comprehend the length evolution in the growth of helical structures. In this report, we derive the analytical expression of the length of helical structures. We then evaluate the correlation between the kinetic length of helical crystals and a number of important parameters including the height, diameter and helical pitch, which are all observable *via* common optical and electronic microscopic techniques. Our investigation is applicable to explain not only the helical growth kinetics at the micro/nano-scale in the materials field, but also the helical growth phenomena in nature in general.

Helical structures are commonly-seen in nature and the intriguing formation as well as the promising properties of such structures has recently triggered extensive research interest.⁸⁻¹³ In particular, various helical micro/nano-scale structures have been prepared and investigated in recent years.^{2-7,11,12} Despite the different growth mechanisms as proposed in the field, it has been unanimously accepted that the specific symmetry, the size and the crystallinity are closely correlated with the intrinsic characteristics of the catalysts employed in the helical growth. 13,14 Such catalyst-growth correlation, yet inadequately addressed, has been elucidated and many insightful growth details have been observed and qualitatively rationalized.¹⁵ Despite such advances, detailed investigation into the kinetic models of helical growth still remains elusive. Such a lag is due to the lack of the analytical investigation into the specific length evolution over time, i.e. the expression of dL/dt, in which L represents the length of the spiral, and t is the growth time of the spiral. To better understand the growth mechanism and efficiently manipulate the growth of helical structures in experiments, the kinetics of helical growth must be revealed quantitatively. In this report, we first demonstrate the viability of our analytical work with actual experimental data of carbon helical nano-fibers grown under different conditions. We then derive the analytical correlation between the length of general helical structures and the parameters associated with these helical structures, all of which are readily obtainable via regular microscopic techniques including scanning electron microscopy (SEM) and transmission electron microscopy (TEM). The quantitative evaluation on the growth mechanism and kinetics of helical structures, enabled for the first time by our present study, opens up the opportunity of analytically understanding the growth of helical structures and exploring their application

The key experimental growth parameters including temperature (T), reaction pressure (P) and reaction time (t), can affect the catalyst properties, which are then determined by the topography and exposed crystal facets of the catalyst particles in the helical growth. Amelinckx et al. proposed a formation mechanism for helical graphite nanotubes by introducing the concept of spatial-velocity hodograph. However, the length evolution of helical carbon fibers in the growth process was not investigated in detail. According to our investigation, the reaction temperature has substantial effect on the growth rate of helical carbon fibers. As the reaction temperature is set at 190 \square , the spiral length reaches a value in the range of 1000 nm- 2800 nm after growing for 60 min at 1 atm, as shown in Figure 1, and the value of dL/dt is in the range of 20 nm/min-56 nm/min. It is also noted that the morphologies of fibers are different, which might be due to the anisotropic catalytic properties of Cu nanocrystals. As reported by Qin et al, the spiral length reaches 3000 nm-5000 nm at 195 \square for 10 min, and the growth rate of coils is in the range of 30 nm/min. In addition, the spiral length can reach 6400 nm-8000 nm at 250 \square for 3 min, and the growth rate of coils increases to 2133 nm/min-2666 nm/min. In that has been revealed that the value of spiral length increases not only in proportion to the reaction temperature and time, but also inversely proportional to the reaction pressure. For instance, by fixing the partial pressure of acetylene at \sim 0.1 atm, the length of the helical carbon fibers approaches the range of 500 nm-800 nm at 271 \square for 10 min.

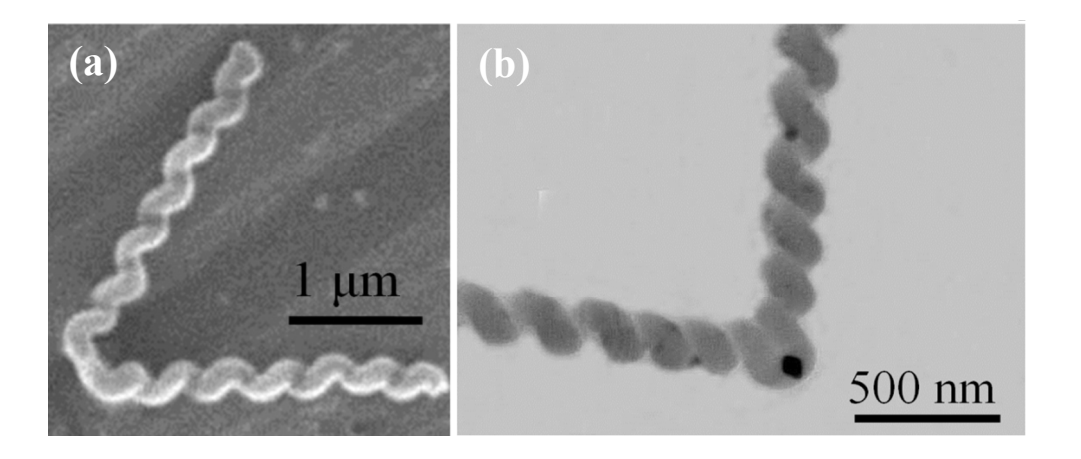


Figure 1 The SEM image (a) and TEM image (b) of a twin helical structure grown on a single Cu nanocrystal at 190 °C for 60 min.

Indeed, the spiral length of helical fibers increases with the temperature, reaction time and reaction pressure. 15 Meanwhile, the growth rate dL/dt is closely correlated with the specific Miller indices of the contacting crystal facets of the catalyst crystal; the higher the Miller-index of the contacted facet is the higher the growth rate for the helical fibers. The diameter of the fibers is determined by the size of the catalyst particles.²⁰ The value of dL/dt decreases as the size of the catalyst particle increases. The growth rate is typically determined by the contact region between the catalyst particles and the already-formed fiber segment. The pitch of the helical fibers (d) is determined by the ratio of the curling rate to the extruding rate of the fiber. As a consequence, the pitch decreases with increasing ratio of the curling rate to extruding rate and vice versa. ¹⁷ With all the aforementioned parameters, one can then evaluate the parameters associated with the growth kinetics of the helical fiber, as shown in Figure 2. In particular, a theoretical derivation and evaluation of L will facilitate such efforts. ^{15,17,20}

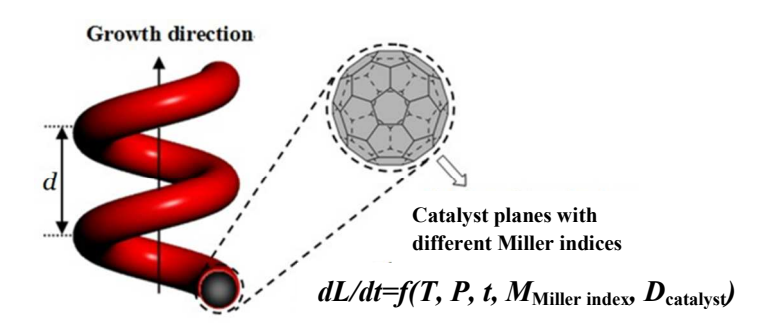


Figure 2 Kinetic model analysis over the spiral length evolution with respect to temperature (T), pressure (P), time (t), Miller index $(M_{\text{Miller index}})$ and the diameter of the catalyst particles (D_{catalyst}) .

The importance for quantitatively evaluating the length evolution for studying the growth mechanism and kinetics of a helical structure can be readily elucidated in the above discussion. We next derive the analytical expressions of the lengths of helical structures. In general, there are two types of helical lines, as shown in Figure 3, in which the one with a cylinder shape is noted as CLHL and the one with a cone shape is noted as COHL, respectively.

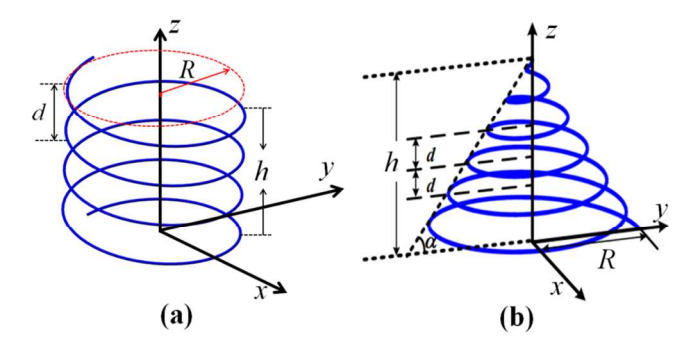


Figure 3 | Helical lines in (a) a CLHL shape, and (b) a COHL shape. In the figure d indicates the pitch, R is the bottom radius, h is the height of the helical structure, and α is the corner angle of the cone.

For the CLHL case, the parametric equations of a cylinder shaped helical line can be written as follows,

$$\begin{cases} x(\theta) = R \cos \theta \\ y(\theta) = R \sin \theta \end{cases}, \quad 0 \le \theta \le 2k\pi,$$

$$z(\theta) = v\theta$$
(1)

where x, y, z are the three axes in a classical Cartesian coordination, θ is the rotation angle of the \vec{R} away from the x axis, $v = \frac{d}{2\pi}$ is the growth rate of the CLHL-shaped helical line along the z axis, and $k = \frac{h}{d}$. Then the helical length of a CLHL (L_{CLHI}) structure can be obtained via Eq. 1,

$$L_{CLHL} = \int_0^{2k\pi} [[x'(\theta)]^2 + [y'(\theta)]^2 + [z'(\theta)]^2]^{1/2} d\theta = \frac{2*h*\pi\sqrt{0.0253303*d^2 + R^2}}{d}$$
(2)

Similarly, the helical length of a COHL (L_{COHL}) structure can also be obtained. The analytical equations for COHL can thus be written as in Eq. 3,

$$\begin{cases} x(\theta) = R(\theta) \cos \theta \\ y(\theta) = R(\theta) \sin \theta, \quad 0 \le \theta \le 2k\pi, \\ z(\theta) = v\theta \end{cases}$$
 (3)

where $R(\theta) = R - v\theta \cot \alpha$, $v = \frac{d}{2\pi}$, and $k = \frac{H}{d}$. Then the length of the spiral line is given by Eq. 4,

$$L_{COHL} = v \int_0^{2k\pi} \left[\theta^2 \cot^2 \alpha - \theta \cot \alpha \frac{2R}{v} + c \right]^{1/2} d\theta$$
 (4)

where $c = 1 + \cot^2 \alpha + \left(\frac{R}{v}\right)^2$. The integration of Eq. 4 is employed to obtain the final integration form of L_{COHL} , as expressed in Eq. 5, where the parameters used are noted in Figure 3(b).

 $L_{COHL} =$

$$\left[\frac{\theta d \cot \alpha - R}{4\pi \cot \alpha} \sqrt{\frac{(4\pi^2 R - dv\theta \cot \alpha)^2}{d^2} + 1 + \cot^2 \alpha} + \frac{d(1 + \cot^2 \alpha)}{4\pi \cot \alpha} \operatorname{arsinh}\left(\frac{d(\theta d \cot \alpha - 2\pi R)}{4\pi^2 \sqrt{1 + \cot^2 \alpha}}\right) \right] \Big|_{0}^{2k\pi}$$
(5)

in which the parameters used are the same with those indicated in Figure 3(b). The detailed integration of Eq. 5 is provided in the Supporting Information.

Since the shape of the helical fibers is determined by the index deviation in the crystalline facets of the catalyst crystal at the contact point where the helical fibers are grown, by employing the facets of certain Miller indices,

certain helical fibers can be obtained. For the case of CLHL, based on Eq. 1 the correlation of $L_{\rm CLHL}$ with parameters of d, R and h are shown in Figure 4. From Figure 4(a), L first decreases rapidly and then the decrease becomes gradual with increasing d until approaching zero. There exists a critical point in the decreasing plots, and the critical point increases with increasing R. For a growing helical fiber with small d before the critical point, the growth rate of the helical fiber decrease abruptly with increasing d, which suggests there is a stress or tension dependent kinetics in the growth of a helical fiber with a small helical pitch.

In addition, the correlation between L_{CLHL} and R/h is also investigated. As shown in Figure 4(b) and Figure S1, L_{CLHL} is linearly dependent on the radius R as well as the height h. For a CLHL with a fixed h, L_{CLHL} increases much faster with increasing R for the CLHL structure with a smaller d, as shown in Figure 4(b). Similarly, for a CLHL structure with a certain diameter R, L_{CLHL} also increases with increasing h in a larger slope for the CLHL structure with a smaller d, as shown in Figure S1. The non-linear dependence of L_{CLHL} on d can also be demonstrated from both Figure 4(b) and Figure S1. As noted in these figures, L_{CLHL} increases slowly in the plots with $d \ge 0.2$, and increases abruptly with d < 0.2 nm as shown in Figure 4(b). This trend is consistent with that shown in Figure 4(a).

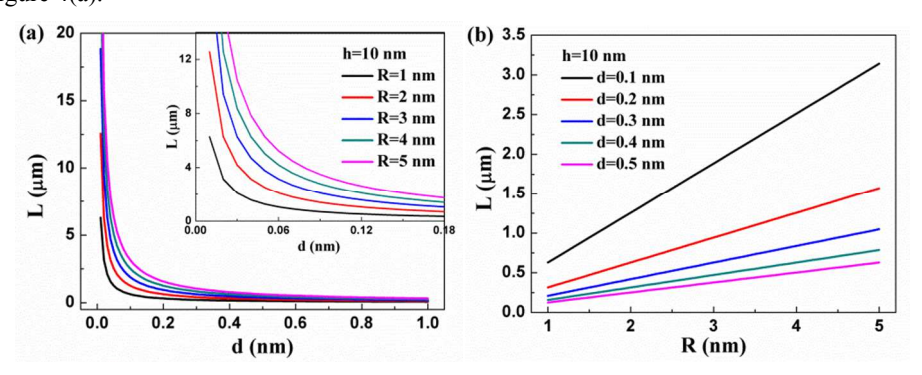


Figure 4 (a) Plots of L_{CLHL} vs. d with fixed R and h, and (b) plots of L_{CLHL} vs. R with fixed h and d.

The shape of the helical fibers is highly dependent on the crystal facets on the growth point of the catalyst. It has been reported that catalyst particles appeared to undergo a further change in shape and rotate around an axis perpendicular to the direction of the filament growth, causing the filament to form a spiral structure. This leads to the change in the morphology of the helical fibers, due to the variation in the Miller indices of the crystal facets of the catalyst.

For the case of COHL based on Eq. 3, the correlation of L_{CLHL} with parameters of d, R and α are shown in Figure 5. Clearly, these plots show different dependences of L_{COHL} on d and R, compared with that in the CLHL structure as shown in Figure 4. Though the dependence of L_{COHL} on d shown in Figure 5(a) is similar with the L_{CLHL} -versus-d plots as shown in Figure 4(a), neither plots of L_{COHL} versus d nor plots of L_{COHL} versus R are linear, as shown in Figure 5(a) and (b). In addition, L_{COHL} increases non-linearly with α , as shown in Figure 5(c). With increasing α , L_{COHL} first increases slowly, and then the increasing slope becomes much steeper as α reaches a critical point. Interestingly, the position of the critical point appears to decrease with decreasing d. Thus, for the COHL case with a smaller d, the length growth of the fiber increases much faster on its axial direction. It also implies that a stress modulates the growth kinetics in the growth of COHL-type helical fibers. The plots of L_{CLHL} vs. h in the COHL case are given in Figure S2, which indicates a linear dependence of L on h.

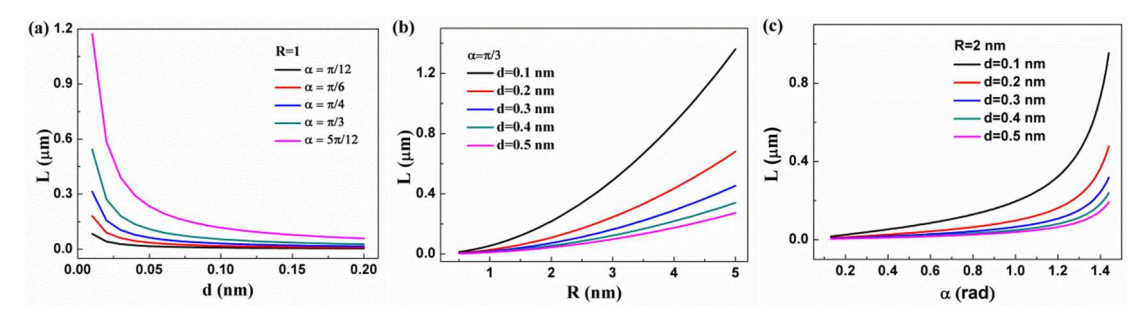


Figure 5 | Length evolution as a function of helical structure parameters for COHL. (a) plots of L_{COHL} vs. d with fixed R and α , (b) plots of L_{COHL} vs. R with fixed α and d, and (c) plots of L_{COHL} vs. α with fixed R and d.

Our quantitative analysis shows that the correlation between the length evolution, *i.e.* the growth kinetics of helical micro/nano materials, and the known parameters associated with the helical growth can be quantitatively investigated. In addition, it is known that different stresses/tensions are present in spirals with different *Rs*, and thus with the length of the spiral, the stress/tension-dependent growth kinetics can be readily investigated. ^{15,20,21} Future studies can focus systematically on correlation of stress/tension *versus* spiral length evolution. Nonetheless, present work inspires further analytical study over the growth mechanism of general helical structures with characterizable kinetics-related parameters. As a consequence, the design of synthetic conditions as well as the pre-evaluation of the helical structures is viable.

Conclusion

In this report, we demonstrate that the kinetic models, despite complexity, can be elucidated with the assessment of length of the helical structure versus growth time. The derived length expressions associated with such growth parameters as the angle, the pitch and the height of the helical structures, facilitates the investigation into the kinetics of helical growth. Our study, combined with microscopy data, is expected to improve the fundamental understanding on the growth mechanism of helical materials, known for their intriguing physical properties and promising application potentials.

Acknowledgements

The work is supported in part by the UESTC new faculty startup fund. Y. Song acknowledges the support from National Natural Science Foundation (grant no. 61106099).

References

- P. Chambon, J. D. Weill, and P. Mandel, Nicotinamide mononucleotide activation of a new DNA-dependent polyadenylic acid-synthesizing nuclear enzyme. Biochem. *Biophys. Res. Comm.* **11**, 39-43, doi: 10.1016/0006-291X(63)90024-X (1963).
- Y. Qin, H. Li, Z. K. Zhang, Z. L. Cui, Symmetric and helical growth of polyacetylene fibers over a single copper crystal derived from copper tartrate decomposition. *Org. Lett.* 4, 3123-3125, doi:10.1021/ol026446x (2002).
- T. Lingham-Soliar, N. Murugan, A new helical crossed-fibre structure of β-Keratin in flight feathers and its biomechanical implications. *Plos One* **8**, 1-12, doi:10.1371/journal.pone.0065849 (2013).
- 4 X. M. Xi, G. K. L. Wong, T. Weiss, and P. St. J. Russell, Measuring mechanical strain and twist using helical photonic crystal fiber. *Opt. Lett.* **38**, 5401-5404, doi:10.1364/OL.38.005401 (2013).
- Y. Y. Cao, J. J. Xie, B. Liu, L. Han and S. N. Che, Synthesis and characterization of multi-helical DNA-silica fibers. *Chem. Commun.* **49**, 1097-1099, doi:10.1039/C2CC37470F (2013).

- A. Miserez, and P. A. Guerette, Phase transition-induced elasticity of α-helical bioelastomeric fibres and networks. Chem. Soc. Rev. 42, 1973-1995, doi:10.1039/C2CS35294J (2013).
- L. Bourgeois, T. Williams, M. Mitome, R. Derrien, N. Kawamoto, D. Golberg, and Y. Bando, Origin of coproduced boron nitride and carbon helical conical fibers. *Cryst. Growth Des.* 11, 3141-3148, doi:10.1021/cg200397z (2011).
- X. Jian, M. Jiang, Z. W. Zhou, Q. Zeng, J. Lu, D. C. Wang, J. T. Zhu, J. H. Gou, Y. Wang, D. Hui, Gas-induced formation of Cu nanoparticle as catalyst for high-purity straight and helical carbon nanofibers. *ACS Nano* 6, 8611-8619, doi:10.1021/nn301880w (2012).
- L. Liu, P. G. He, K. C. Zhou, T. F. Chen, Microwave absorption properties of helical carbon nanofibers-coated carbon fibers. AIP Advances 3, 082112, doi:10.1063/1.4818495 (2013).
- 10 X. M. Xi, G. K. L. Wong, T. Weiss, P. S. Russell, Measuring mechanical strain and twist using helical photonic crystal fiber. *Opt. Lett.* 38, 5401-5404, doi:10.1364/OL.38.005401 (2013).
- 11 C. N. Alexeyev, B. P. Lapin, A. V. Volyar, M. A. Yavorsky, Helical-core fiber analog of a quarter-wave plate for orbital angular momentum. *Opt. Lett.* **38**, 2277-2279, doi:10.1364/OL.38.002277 (2013).
- H. Kim, J. Kim, Y. Jung, L. A. Vazquez-Zuniga, S. J. Lee, G. Choi, K. Oh, P. Wang, W. A. Clarkson, Y. Jeong, Simple and reliable light launch from a conventional single-mode fiber into a helical-core fiber through an adiabatically tapered splice. *Opt. Express* **20**, 25562-25571, doi:10.1364/OE.20.025562 (2012).
- N. J. Tang, J. F. Wen, Y. Zhang, F. X. Liu, K. J. Lin and Y. W. Du, Helical Carbon Nanotubes: Catalytic Particle Size-Dependent Growth and Magnetic Properties. *ACS Nano* **4**, 241-250, doi:10.1021/nn901425r (2010).
- B. Toboonsung, S. Pisith, Growth conditions for carbon nanotubes and helical nanofibers on copper substrates using sparked catalysts. *Adv. Mat. Res.* **55**, 561-564, doi:10.4028/www.scientific.net/AMR.55-57.561 (2008).
- R. P. Gao, Z. L. Wang, and S. S. Fan, Kinetically controlled growth of helical and zigzag shapes of carbon nanotubes. *J. Phys. Chem. B* **104**, 1227-1234, doi: 10.1021/jp9937611 (2000).
- S. Amelinckx, X. B. Zhang, D. Bernaerts, X. F. Zhang, V. Ivanov, J. B. Nagy, A formation mechanism for catalytically grown helix-shaped graphite nanotubes. *Science* **265**, 635-9, doi: 10.1126/science.265.5172.635 (1994).
- X. Jian, D. C. Wang, H. Y. Liu, M. Jiang, Z. W. Zhou, J. Lu, X. L. Xu, Y. Wang, L. Wang, Z. Z. Gong, M. L. Yang, J. H. Gou, D. Hui, Controllable synthesis of carbon coils and growth mechanism for twinning double-helix catalyzed by Ni nanoparticle. *Composites: Part B* In Press, doi: 10.1016/j.compositesb.2013.06.010 (2013).
- Y. Qin, L. Y. Yu, Y. Wang, G. C. Li, Z. L. Cui, Amorphous helical carbon nanofibers synthesized at low temperature and their elasticity and processablity. *Solid State Commun.* **138**, 5-8, doi:10.1016/j.ssc.2006.01.048 (2006).
- Y. Qin, Q. Zhang, Z. L. Cui, Effect of synthesis method of nanocopper catalysts on the morphologies of carbon nanofibers prepared by catalytic decomposition of acetylene. *Journal of Catalysis* **223**, 389-394, doi: 10.1016/j.jcat.2004.02.004 (2004).
- N. M. Rodriguez, A review of catalytically grown carbon nanofibers. *J. Mater. Res.* 8, 3233-3250, doi: 10.1557/JMR.1993.3233 (1993).
- M. J. Behr, K. A. Mkhoyan, E. S. Aydil, Catalyst rotation, twisting, and bending during multiwall carbon nanotube growth. *Carbon* 48, 3840-3845, doi: 10.1016/j.carbon.2010.06.049 (2010).
- M. Kim, N. Rodriguez, R. Baker, The role of interfacial phenomena in the structure of carbon deposits. *Journal of Catalysis* **134**, 253-268, doi: 10.1016/0021-9517(92)90226-8 (1992).